RESEARCH ARTICLE

Solvent-Free Melt Electrospinning for Preparation of Fast Dissolving Drug Delivery System and Comparison with Solvent-Based Electrospun and Melt Extruded Systems

ZSOMBOR KRISTÓF NAGY,[1] ATTLIA BALOGH,[1] GÁBOR DRÁVAVÖLGYI,[1] JAMES FERGUSON,[2] HAJNALKA PATAKI,[1] BALÁZS VAJNA,[1] GYÖRGY MAROSI[1]

[1]Organic Chemistry and Technology Department, Budapest University of Technology and Economics, Budapest H-1111, Hungary

[2]School of Engineering, The University of Edinburgh, Edinburgh EH9 3JL, United Kingdom

Received 13 August 2012; revised 18 October 2012; accepted 24 October 2012

Published online in Wiley Online Library (wileyonlinelibrary.com). DOI 10.1002/jps.23374

ABSTRACT: The solvent-free melt electrospinning (MES) method was developed to prepare a drug delivery system with fast release of carvedilol (CAR), a drug with poor water solubility. To the authors knowledge, this is the first report for preparing drug-loaded melt electrospun fibers. Cationic methacrylate copolymer of Eudragit® E type was used as a fiber forming polymer matrix. For comparison, ethanol-based electrospinning and melt extrusion (EX) methods were used to produce samples that had the same composition as the melt electrospun system. According to the results of scanning electron microscopy, X-ray diffraction, differential scanning calorimetry, and Fourier transformed infrared spectrometry investigations, amorphous solid nanodispersions/solutions of CAR in Eudragit® E matrix were obtained in all cases with 20 $^{m}/_{m}$% drug content. *In vitro* drug release in acidic media from the extrudates was significantly faster (5 min) than that from crystalline CAR. Moreover, ultrafast drug release was achieved from the solvent-free melt and ethanol-based electrospun samples because of their huge surface area and the soluble polymer matrix in the acidic media. These results demonstrate that solvent-free MES is a promising, novel technique for the production of drug delivery systems with enhanced dissolution because it can combine the advantages of EX (e.g., solvent-free, continuous process, and effective amorphization) and solvent-based electrospinning (huge product surface area). © 2012 Wiley Periodicals, Inc. and the American Pharmacists Association J Pharm Sci

Keywords: melt electrospinning; oral drug delivery; amorphous; electrospun nanofibers; extrusion; solid dispersion; solid solution; enhanced dissolution rate; continuous pharmaceutical manufacturing

INTRODUCTION

There is a continuously increasing demand for developments in convenient methods to create drug delivery systems with controlled dissolution of the active pharmaceutical ingredient (API). Sustained drug release is generally needed in the case of drug-loaded implants,[1] tissue scaffolds (tissue engineering),[2] and wound dressings[3] to attain an adequate long-term effect. However, in the case of oral dosage forms, enhanced dissolution is often required, in addition to sustained drug release,[4–6] to achieve sufficient bioavailability.[7] It is a significant challenge for pharmaceutical technologists because of the increasing number of drugs with poor water solubility.[8,9]

Solid micro- and nanodispersions, or even solid solution, are some of the most promising strategies to improve drug dissolution.[10–15] The potential of solvent-free melt extrusion (EX) to increase the drug dissolution rate has been demonstrated by numerous papers,[16–22] and marketed products prepared by this method (e.g. Kaletra® and Isoptin-SRE® (Abbott, Chicago, Illinois)).[23] Formation of nanofibers by electrospinning technique from drug-containing polymer solutions has been introduced recently as a technique capable of enhancing the dissolution rate of drugs.[24–31] This is because of several factors, including the formation of an amorphous solid solution, the

Correspondence to: Zsombor K. Nagy (Telephone: +36-1-4631424; Fax: +36-1-4633648; E-mail: zsknagy@oct.bme.hu)

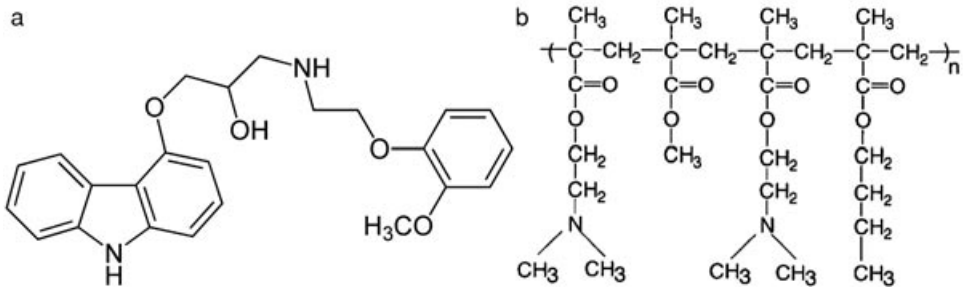

Scheme 1. Formula of (a) carvedilol and (b) Eudragit® E.

huge surface area produced, and good solubility of the matrix forming polymer.[30]

Electrospinning was originally applied in the textile and filtration industry.[32–36] Later on, medical research has been carried out in the field of wound dressing[37] and tissue engineering.[38,39] A relatively low number of publications can be found in the literature about the application of melt electrospinning (MES) compared with solution electrospinning (SES).[40] This may be due to the complexity of MES compared with SES.

The first scientific paper about MES was published in 1981, it described how polyethylene and polypropylene melts were electrospun.[41] Later, several other water-insoluble polymers (e.g., polylactic acid,[42] poly(lactic-*co*-glycolic) acid,[43] polycaprolactone,[44] polyethylene terephthalate,[45] poly(methyl methacrylate,[46] and thermoplastic polyurethane[47]) were melt electrospun successfully forming micro- and nanofibers. The literature of the field of MES has recently been reviewed by Hutmacher and Dalton.[40]

Melt electrospinning has several advantages over SES. There is no need to dissolve the fiber forming polymer, there is no need for expensive solvent recovery, there is no risk of solvent explosion, there is no residual solvent in the fibers, and a quantitative yield (100%) is achievable. Generally, MES is a safer and "greener" technology than organic-solvent-based electrospinning. These aspects have increasing importance in the pharmaceutical industry. Another important technological advantage of MES is that it can be coupled with EX and thus continuous manufacturing is feasible, as shown by Lyons et al.[48] and Malakhov et al.[49]

In spite of these obvious advantages, the solvent-free MES has not yet been applied for preparing novel drug delivery systems (neither for pharmaceutical, nor for tissue engineering). It seemed to us promising to combine the advantages of pharmaceutical EX (e.g., solvent-free, continuous process, and effective amorphization) and solvent-based electrospinning (e.g., huge product surface area) this way for achieving enhanced dissolution.

Thus, the aim of this work was to investigate the applicability of MES to improve drug dissolution of a model drug with poor water solubility (CAR) by preparing fast dissolving formulations and comparing it with solution electrospun and melt extruded formulations with the same composition.

MATERIALS AND METHODS

Materials

Carvedilol (CAR, Scheme 1) from Sigma–Aldrich (Budapest, Hungary) with purity ≥98% was used in this work. The melting point of CAR is 117°C.[22] Eudragit® E PO (Eudragit® E, E PO, Scheme 1) was kindly provided by Evonik (Darmstadt, Germany), which is a butylmethacrylate–(2-dimethylaminoethyl) metachrylate–methylmethacrylate copolymer (1:2:1). It is an amorphous polymer with an average molecular weight of about 150,000 g/mol.

Melt Extrusion

Reference solid dispersion of Eudragit® E and CAR (20%) was prepared by HAAKE MiniLab micro compounder (Thermo-Haake, Karlsruhe, Germany) for comparison with the electrospun fibers. Dry premix (mixed with pestle in a mortar) of API and the polymer was introduced into the hopper of a mini extruder. The temperature and rotation speed was fixed at 130°C and 20 rpm, respectively, and no recirculation was applied. The extrudates obtained were ground before the dissolution tests by IKA MF10 microfine grinder equipped with a MF 10.2 impact grinding head (Staufen, Germany). The sieve used was MF 2.0 mm, and the rotation speed was 3000 rpm.

Solvent-Based Electrospinning

The polymer was added to ethanol and stirred by a magnetic stirrer (600 rpm, 50°C) until completely dissolved. The API was dissolved in the polymer solution (magnetic stirrer, 600 rpm), which was introduced into the electrostatic spinner. The electrostatic spinning unit was equipped with a NT-35 high-voltage DC supply (MA2000, Nagykanizsa, Hungary). The

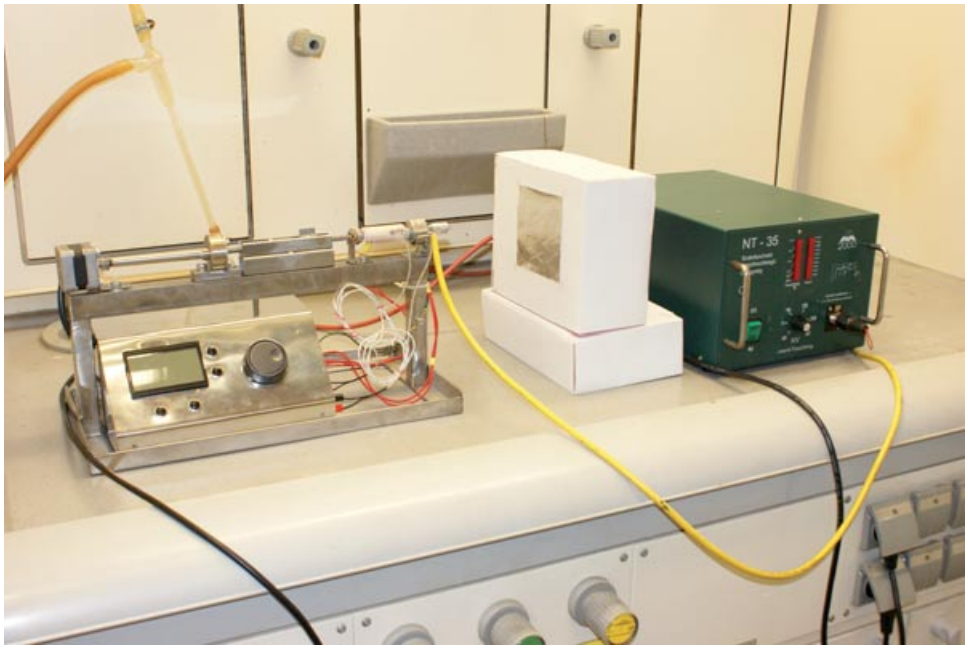

Figure 1. The photograph of the melt electrospinning apparatus.

electrical potential on the spinneret electrode was adjusted during the experiments between 20 and 25 kV. A grounded aluminum plate covered with aluminum foil was used as collector. The distance between the spinneret and the collector was 15 cm, and the experiments were performed at room temperature (25°C). Polymer solution was dosed by SEP-10S Plus syringe pump (Aitecs, Vilnius, Lithuania).

Melt Electrospinning

Melt-homogenized drug–polymer mixture was fed into MES equipment, which was designed and built at Department of Organic Chemistry and Technology, Budapest University of Technology and Economics (Budapest, Hungary). The MES equipment (Fig. 1) has two temperature-controlled zones and a programmable feeder of melts or solutions. The temperature and the feeding rate were controlled by a Microchip® microcontroller (Microchip Technology, Chandler, Arizona), which was programmed by MPLAB MCC18 student edition compiler (Microchip Technology, Chandler, Arizona). The stainless steel metal syringe is easily dismountable and the melts or the solutions can be washed away by an appropriate flushing liquid. The material remaining in the needle of the syringe can be melt away or drilled through before the flushing, if it is needed. The applied feeding rate was 0.5 mL/h and temperatures T_B and T_A were set at 130°C and 155°C, respectively (Fig. 2). The electric potential on the collector electrode was set to 35 kV, and the spinneret was grounded. The distance of the spinneret and the collector was 10 cm.

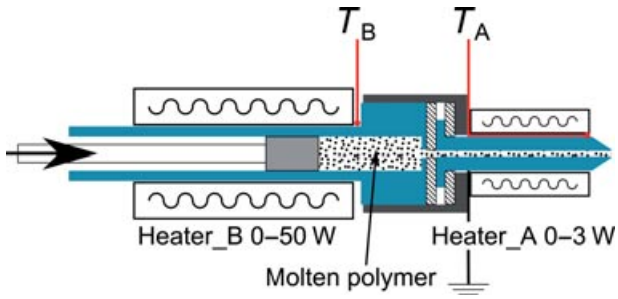

Figure 2. The drawing of the two-zone-heated stainless steel metal syringe.

Differential Scanning Calorimetry

Differential scanning calorimetry (DSC) measurements were carried out using a Setaram (Calure, France) DSC 92 apparatus (sample weight: ~10–15 mg, open pan, nitrogen flush). The temperature program consisted of an isothermal period, which lasted for 1 min at −30°C (with liquid nitrogen cooling), with subsequent linear heating from −30°C to 300°C at the rate of 10°C/min.

Scanning Electron Microscopy

Morphology of the samples was investigated by a JEOL 6380LVa (JEOL, Tokyo, Japan) type scanning electron microscope. Each specimen was fixed by conductive double-sided carbon adhesive tape. The applied accelerating voltage and working distance were between 15 and 30 kV and 10 and 12 mm, respectively.

Fourier Transformed Infrared Spectrometry

The KBr tablet sample preparation method was used for the Fourier transform infrared (FTIR) spectrometric measurements of untreated materials, ground extrudate, and electrospun samples. The obtained tablets were analyzed by Bruker Tensor 37 type spectrometer equipped with a deuterated triglycine sulfate detector (Ettlingen, Germany) in the range of 4000–400 cm^{-1} with a resolution of 4 cm^{-1}.

X-Ray Diffraction

Powder X-ray diffraction (XRD) patterns were recorded by a PANanalytical X'pert Pro MDP X-ray diffractometer (Almelo, The Netherlands) using Cu-Kα radiation (1.542 Å) and a Ni filter. The applied voltage was 40 kV, whereas the current was 30 mA. The untreated materials, the physical mixture (mixed using a mortar and pestle), the ground extrudate, and the electrospun samples were analyzed for angles 2θ between 2° and 42°.

In Vitro Dissolution Measurement

The dissolution studies were performed using an Erweka DT6 dissolution tester (USP II apparatus, Heusenstamm, Germany). Samples equivalent to 12.5 mg of CAR were added in the dissolution vessel containing 900 mL 0.1 M HCl maintained at 37 ± 0.5°C and stirred at 50 rpm. Untreated CAR and the ground extrudate were added as a powder, and the electrospun samples were added as a nonwoven sheet directly in the vessel. Samples (5 mL) were collected periodically and the concentration of CAR was determined by a HP 8452 UV spectrophotometer (Hewlett-Packard, Palo Alto, California) using a diode array detector at 242 nm. Percentage of dissolution was readily calculated according to the calibration curves of CAR in 0.1 M HCl because of the lack of absorption peaks of Eudragit® E in this range.

RESULTS AND DISCUSSION

The literature of MES provided information only about water-insoluble polymers without drug content processed this way. Therefore, several questions needed to be answered in this work: what is the feasibility of water-soluble fiber formation by means of MES, what is the structure of drug-containing polymers produced this way, how effective is the amorphization during the MES process comparing with other methods, and how it improves the dissolution? At first, the process parameters and the obtained morphologies were investigated to map the advantages and disadvantages of MES compared with SES and EX.

Comparison of the SES, MES, and Extrusion Processes and the Obtained Morphologies

A common polymer matrix was required for comparing the three continuous processes. Eudragit® E, a thermoplastic amorphous polymer, was selected as a dissolution enhancing matrix. Eudragit® E dissolves in water-based media if the pH is below 5 (like in the stomach) because of the protonation of the dimethylamino-ethyl groups. In a previous work, it was demonstrated that Eudragit® E has good compatibility with CAR and it is able to stabilize this drug in amorphous state.[21]

In the case of SES, the optimal polymer content for fiber formation was determined in ethanol (1 g/4 mL) and the same polymer–ethanol ratio were applied when the drug containing SES (0.25 g CAR/1 g Eudragit® E/4 mL ethanol) was performed. The extrusion of Eudragit® E (80%) and CAR (20%) was carried out at 130°C (further circumstances are given in the section "*Materials and Methods*"). During the MES process, the temperature of the feeder was 130°C (T_B), whereas the temperature of the spinneret was 155°C (T_A). This was to achieve lower melt viscosity for adequate fiber formation utilizing the electrostatic forces. The productivity of SES and MES with single needle was significantly lower than that of EX (Table 1). However, the productivity of electrospinning can be drastically improved using recently developed fiber generators instead of single needle.[50,51] Entirely continuous production is feasible using an extruder as a continuous homogenizer and melt feeder.

Several factors were found to favor drug amorphization. In the case of SES, this included dissolution of CAR and fast evaporation of ethanol.[52] In the case of EX and MES, the melting of CAR and fast cooling of the melts (EX and MES) were advantageous. Useful information can be gathered about the amorphization from the obtained morphology of the samples. Smooth surfaces, lack of visible crystals, and inhomogeneties are all indicators of amorphization.

The morphologies of extruded and electrospun samples are shown in Figures 3–5. MES fibers were produced with diameters of 5–30 μm, which is similar to the diameter of other MES fibers prepared from other polymers.[39] The diameters of prepared SES fibers were in the nano range (300–1000 nm) because of the lower viscosity and slower solidification (longer time for elongation).[53] Fine fibers provide huge specific surface area, which is promising from the aspect of dissolution improvement according to the Noyes–Whitney equation. The specific surface area of SES fibers is nearly two orders of magnitude larger than that of the MES fibers because of the difference in fiber diameters (Table 1). In the case of the ground extrudate, SEM images revealed irregularly shaped particles. The diameter of the majority of fibers was between

Table 1. Compositions, Production Process, Diameter, and Specific Surface Area of the Prepared Samples

Sample	Production Process	CAR (mass, %)	EPO (mass, %)	Polymer–Ethanol Ratio (g/mL)	Temperature (°C)	Flow Rate (mL/h)	Productivity (g/h)	Mean Fiber or Particle Diameter (μm)	Specific Surface Area (m^2/g)[a]
EX	Extrusion	20	80	–	130	46	60	250	0.018[b]
SES	Solvent-based electrospinning	20	80	0.25	25	6	1.7	0.7	4.4
MES	Melt electrospinning	20	80	–	155	0.5	0.65	20	0.15

[a] Calculated based on the particle sizes and fiber diameters characterized by scanning electron microscopy.
[b] Calculated as spherical particles.

50 and 1500 μm. The specific surface area of the ground extrudate was one order of magnitude smaller than that of the melt electrospun sample (Table 1). The difference in the specific surface can have significant effect on the dissolution time, which was desired to diminish significantly.

Differential Scanning Calorimetry

Differential scanning calorimetry was applied to investigate the thermal behavior of the samples. For comparison, the pure Eudragit® E and the physical mixture of Eudragit® E with 5% CAR were examined. The DSC curve of the physical mixture shows the (relatively sharp) melting peak of CAR at 120°C and a slightly broader endothermic peak at the glass transition of Eudragit® E (~60°C) (Fig. 6). The melting peak of CAR does not appear in the DSC curves of the extruded and electrospun samples, indicating that the drug is in amorphous form. Extrusion and MES were carried out over the melting point of CAR, which may have helped to totally amorphize CAR. In the case of SES, the process has a very efficient amorphization effect because of the ultrafast evaporation of the solvent, which generally results in a solid solution of the API in the polymer matrix.[29] In the DSC curves of the extruded and electrospun samples, the endothermic peak of glass transition appears at a lower temperature (40°C), which indicates an interaction between CAR and Eudragit® E at the molecular level. CAR acts as a plasticizer in these samples and decreases the polymer–polymer interactions; thus, the segments of the polymer can start to move at a lower temperature. The extrudate and the electrospun samples produced similar DSC curves, indicating the very similar molecular structure of these samples.

Fourier Transform Infrared Spectrometry

The extruded and electrospun samples were investigated by FTIR spectrometry to check the physical and chemical state of the components and their potential degradation under the processing conditions. The obtained results are shown in Figure 7. The spectra of the extrudate and electrospun fibers seem to be a combination of the spectra of the untreated pristine components and no new peak could be detected. It suggests that no detectable decomposition occurred during the extrusion and the electrospinning processes.

Carvedilol has two common polymorphic crystalline forms (Form I and Form II).[54] CAR Form II has one strong band at ~3340 cm^{-1}, whereas Form I displays two strong bands at ~3250 and 3450 cm^{-1}. These are in the absorption region of the O–H and N–H stretching vibrations. Eudragit® E has only two weak and board peaks in this region.

In the spectra of the prepared Eudragit® E–CAR samples, beside the peaks of CAR appearing around

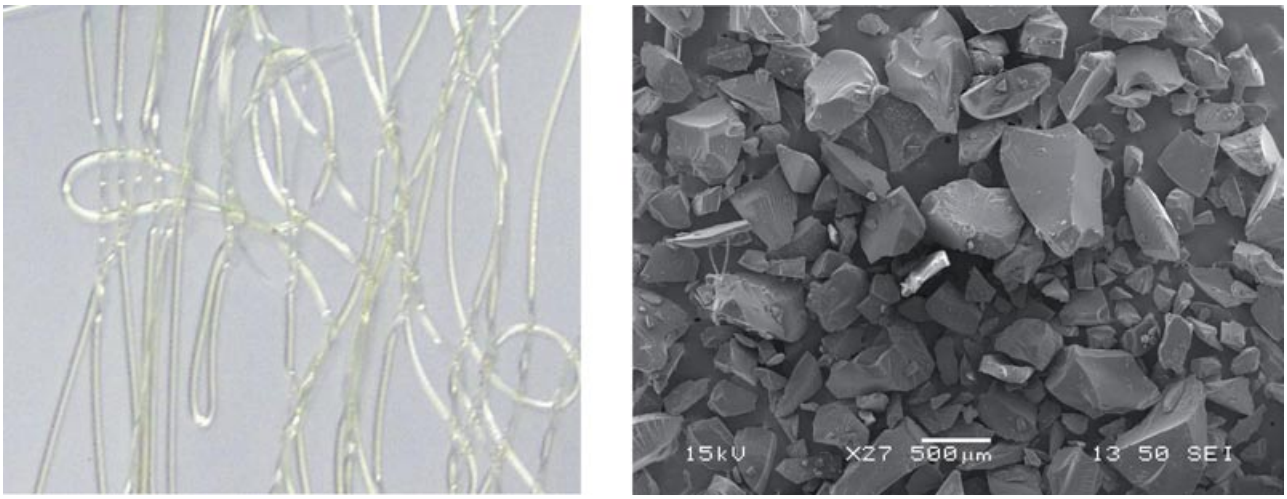

Figure 3. Photo of raw extruded Eudragit® E with 20% carvedilol and scanning electron microscopic image of ground extrudate, magnification: 27×.

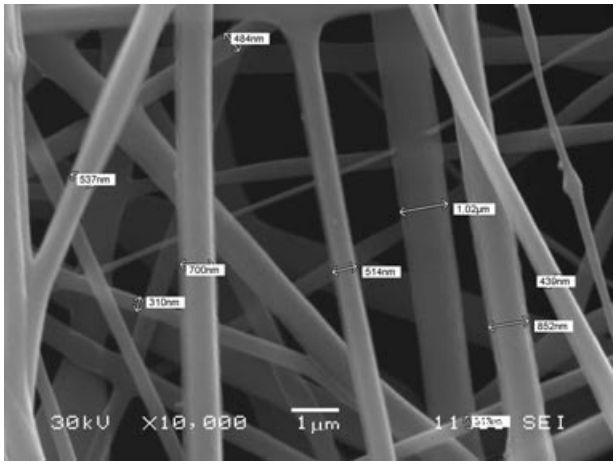

Figure 4. Scanning electron microscopic image of solvent-based electrospun fibers containing Eudragit® E and 20% carvedilol, magnification: 10,000×.

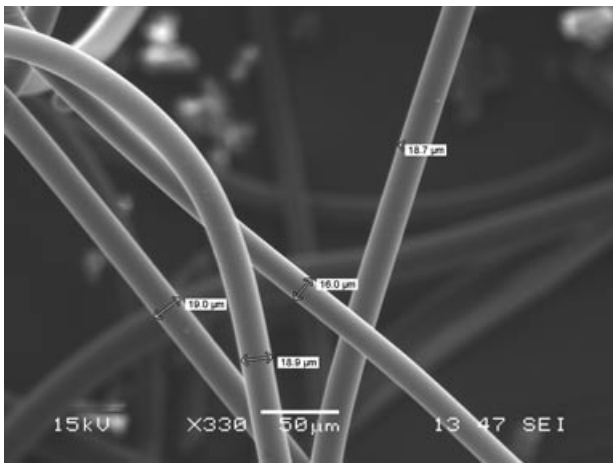

Figure 5. Scanning electron microscopic image of melt electrospun fibers containing Eudragit® E and 20% carvedilol, magnification: 330×.

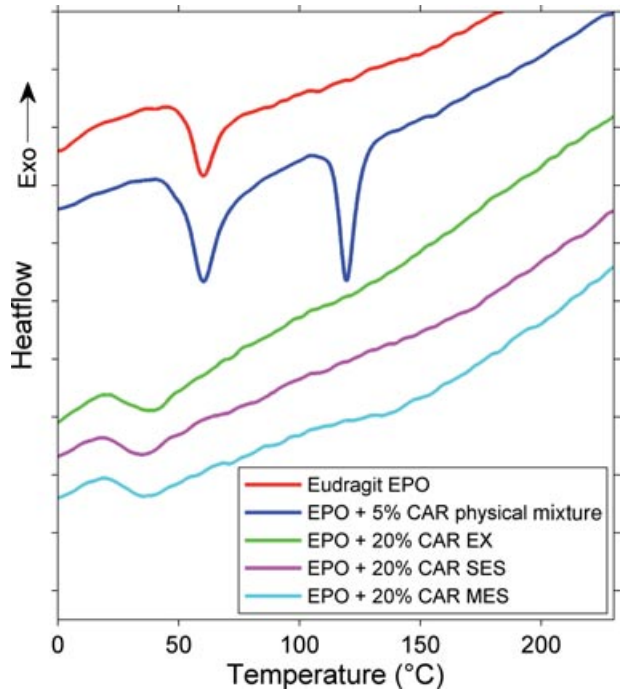

Figure 6. Differential scanning calorimetry curves of pure Eudragit® E, physical mixture of Eudragit® E and 5% carvedilol, extruded sample with 20% carvedilol, solvent-based electrospun fibers (SES) and melt electrospun (MES) fibers with 20% carvedilol.

1600 cm^{-1}, one broader peak was observable from ~3300 to 3450 cm^{-1}, which demonstrates the intermolecular interaction between the Eudragit® E and CAR. It suggests that the CAR is not in crystalline form because the characteristic peaks of crystalline phases of the drug (Form I and Form II) are not present in the spectra. The broad peak indicates its presence in amorphous form. Broadening is due to the various neighborhoods of these bonds, which

 DOI 10.1002/jps

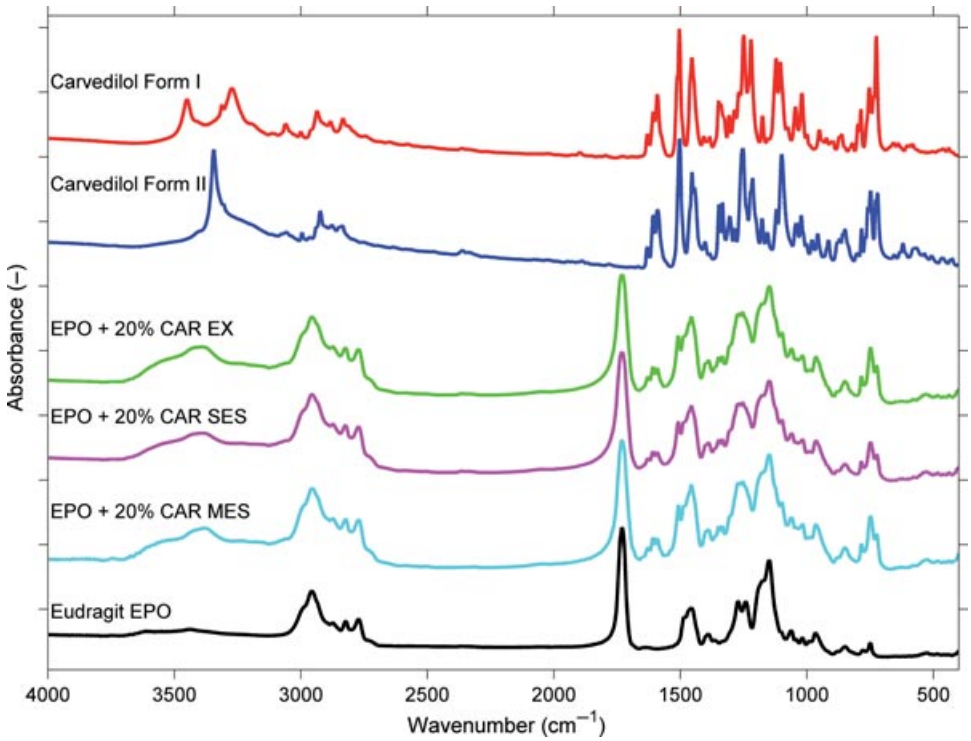

Figure 7. FTIR spectra of crystalline carvedilol (Form I and Form II), extrudate with 20% carvedilol, solvent-based electrospun fibers, melt electrospun fibers with 20% carvedilol and pure Eudragit® E.

perturb the vibrational energies of the bonds compared with the molecules in crystalline phase where the neighborhood of the bonds is uniform (owing to the arranged and repetitive structure of CAR crystals). This deduction corresponds to the results published by Pokharkar et al.[55] The characteristic peaks of CAR at ~750 and 1600 cm^{-1} (Ref. [56]) had significantly lower relative intensities (compared with the characteristic peaks of Eudragit® E) in the spectrum of SES in comparison with the spectra of EX and MES. This phenomenon can be explained by the better distribution of CAR in the polymer matrix because of the better mixing of the two components in solution and the increased sample–air interface (specific surface area Table 1). In general, both the better distribution and the increased sample–air interface may increase the band broadening, which decreases the peak intensities.[57]

Further analyses were made by XRD to confirm that CAR is really in amorphous form in the samples.

X-Ray Diffraction

X-ray diffraction was used to characterize the morphological changes of CAR induced by extrusion and electrospinning. The plots of the EX, SES, and MES samples were compared with those of the individual components and their physical mixtures (Fig. 8). Although CAR preserved its Form II polymorphic structure in the physical mixtures, there was no sharp crystalline peak observed in the XRD patterns of Eudragit® E–CAR samples. These results suggest that CAR was fully transformed to an amorphous form when extruded and electrospun with amorphous Eudragit® E matrix.

On the basis of earlier published results regarding the extruded mixture (e.g., Raman mapping)[21] and the obtained results from FTIR, XRD, and especially from DSC, physical structures of the extruded and the electrospun samples were similar; all of them were very fine solid dispersions/solid solutions.

In Vitro Dissolution

The release profiles of CAR from different forms comparing with the reference are shown in Figure 9. The drug dissolution rate of both extruded and electrospun samples was significantly faster than that of the crystalline CAR. The faster dissolution rate can be attributed to the following factors: although Eudragit® E is not soluble in water-based media if the pH (of the media) is higher than 5, it dissolves rapidly in acidic media such as stomach fluid because of the protonation of amino groups of the polymer chains. The formation of ammonium ions with positive charge and the repulsive (Coulomb) forces within and among the chains accelerate the dissolution of the polymer. CAR molecules dissolve simultaneously with the Eudragit® E matrix because the drug, being in amorphous form, does not need any additional

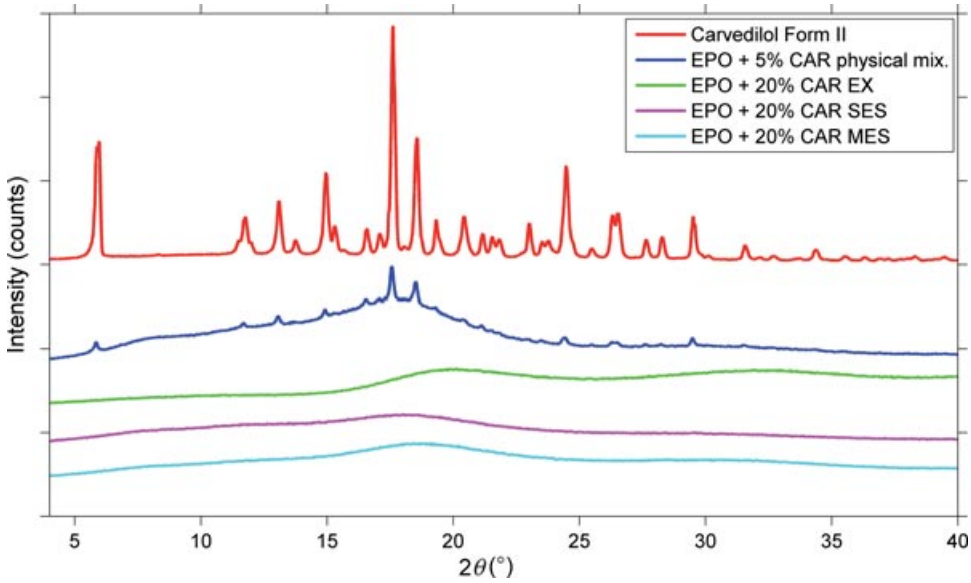

Figure 8. X-ray diffractograms of crystalline carvedilol (Form II), physical mixture of Eudragit® E containing 5% carvedilol, extrudate containing 20% carvedilol, solvent-based electrospun and melt electrospun fibers containing 20% carvedilol.

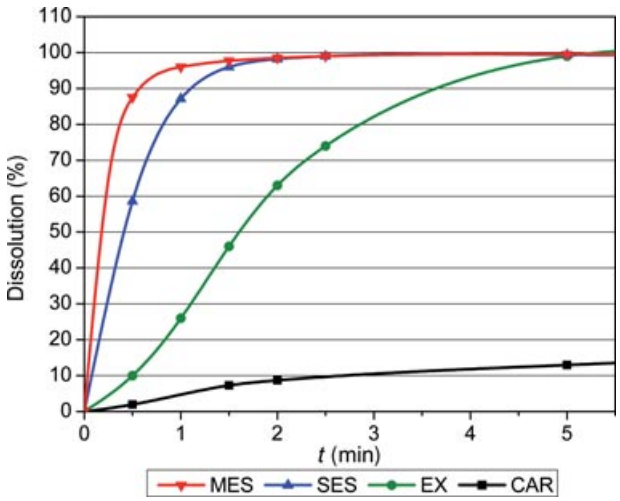

Figure 9. *In vitro* dissolution of carvedilol (CAR) [12.5 mg dosage, 900 mL 0.1 M HCl, USP Dissolution Apparatus 2 (paddle), 50 rpm, 37°C, $n = 3$]. MES, melt electrospun Eudragit® E-based fibers with 20% carvedilol content; SES, solvent-based electrospun Eudragit® E-based fibers with 20% carvedilol content; EX, Eudragit® E-based extrudates with 20% carvedilol; CAR, unprocessed crystalline carvedilol.

action to overcome the crystal lattice energy. It is consistent with the deduction that CAR is molecularly dispersed in the Eudragit® E matrix.

The ground extrudate gave complete release of CAR within 5 min. For MES and SES samples, it took 1 min to dissolve more than 85% of the drug content and another 1 min for complete drug release. In the case of MES, the initial rate of release was faster than SES. This can be explained by the less efficient solvent accessibility of the tightly packed SES fibers, and the increased hydrophobicity induced by CAR. Thus, the accelerating effect of the huge surface area was not fully exploited, despite the fact that SES has nearly two orders of magnitude larger specific surface area than MES. In contrast, the MES sample had a loosely packed nonwoven mat structure, thus the accessibility of the dissolution medium is higher. Although SES had slower dissolution behavior than expected, it was found that the specific surface area of MES and EX samples is proportional to the initial rate of drug release, in accordance with Noyes–Whitney equation. Specific surface area: 1500 cm^2/g (MES) and 180 cm^2/g (EX), initial rate of release: 175%/min (MES) and 20%/min (EX)—the ratio is approximately 8.5 in both cases.

CONCLUSIONS

Novel solvent-free MES method was applied to prepare drug-loaded amorphous Eudragit® E fibers with ultrafast release of CAR, a drug with poor water solubility. The drug release rate of the melt electrospun fibers was significantly higher than that of the ground extrudate with the same composition due to the increased specific surface area. These results demonstrate that solvent-free MES is a promising, novel technique for the production of drug delivery systems with enhanced dissolution because it can combine the advantages of EX (e.g., solvent-free, continuous process, and effective amorphization) and solvent-based electrospinning (e.g., huge product surface area). The productivity of MES with single needle was limited,

however, it can be significantly improved using multi-needle spinning heads or needleless electrospinning method. Further investigation is in progress regarding the deeper understanding of the MES process including the relationship between the melt viscosity and processability.

ACKNOWLEDGMENTS

This work is connected to the scientific program of the "Development of quality-oriented and harmonized R+D+I strategy and functional model at BME" project. This project is supported by the New Széchenyi Plan (project ID: TÁMOP-4.2.1/B-09/1/KMR-2010-0002).

REFERENCES

1. Weinberg BD, Blanco E, Gao J. 2008. Polymer implants for intratumoral drug delivery and cancer therapy. J Pharm Sci 97:1681–1702.
2. Kretlow JD, Klouda L, Mikos AG. 2007. Injectable matrices and scaffolds for drug delivery in tissue engineering. Adv Drug Deliv Rev 59:263–273.
3. Boateng JS, Matthews KH, Stevens HNE, Eccleston GM. 2008. Wound healing dressings and drug delivery systems: A review. J Pharm Sci 97:2892–2923.
4. Higuchi T. 1963. Mechanism of sustained-action medication. Theoretical analysis of rate of release of solid drugs dispersed in solid matrices. J Pharm Sci 52:1145–1149.
5. Kállai N, Luhn O, Dredan J, Kovacs K, Lengyel M, Antal I. 2010. Evaluation of drug release from coated pellets based on isomalt, sugar, and microcrystalline cellulose inert cores. AAPS Pharm Sci Tech 11:383–391.
6. Luhn O, Kallai N, Nagy ZK, Kovacs K, Fritzsching B, Klebovich I, Antal I. 2012. Dissolution profile of novel composite pellet cores based on different ratios of microcrystalline cellulose and isomalt. J Pharm Sci 101:2675–2680.
7. Sugano K, Okazaki A, Sugimoto S, Tavornvipas S, Omura A, Mano T. 2007. Solubility and dissolution profile assessment in drug discovery. Drug Metab Pharmacokinet 22:225–254.
8. Keseru GM, Makara GM. 2009. The influence of lead discovery strategies on the properties of drug candidates. Nat Rev Drug Discov 8:203–212.
9. Lipinski CA. 2000. Drug-like properties and the causes of poor solubility and poor permeability. J Pharm Toxicol Methods 44:235–249.
10. Van den Mooter G. 2011. The use of amorphous solid dispersions: A formulation strategy to overcome poor solubility and dissolution rate. Drug Discov Today 9:79–85.
11. Szuts A, Lang P, Ambrus R, Kiss L, Deli MA, Szabo-Revesz P. 2011. Applicability of sucrose laurate as surfactant in solid dispersions prepared by melt technology. Int J Pharm 410:107–110.
12. Vajna B, Farkas I, Farkas A, Pataki H, Nagy ZK, Madarasz J, Marosi G. 2011. Characterization of drug–cyclodextrin formulations using Raman mapping and multivariate curve resolution. J Pharm Biomed Anal 56:38–44.
13. Rodier E, Lochard H, Sauceau M, Letourneau JJ, Freiss B, Fages J. 2005. A three step supercritical process to improve the dissolution rate of Eflucimibe. Eur J Pharm Sci 26:184–193.
14. Allesų M, Chieng N, Rehder S, Rantanen J, Rades T, Aaltonen J. 2009. Enhanced dissolution rate and synchronized release of drugs in binary systems through formulation: Amorphous naproxen–cimetidine mixtures prepared by mechanical activation. J Control Release 136:45–53.
15. Alonzo DE, Gao Y, Zhou D, Mo H, Zhang GGZ, Taylor LS. 2011. Dissolution and precipitation behavior of amorphous solid dispersions. J Pharm Sci 100:3316–3331.
16. Verreck G, Six K, Van den Mooter G, Baert L, Peeters J, Brewster ME. 2003. Characterization of solid dispersions of itraconazole and hydroxypropylmethylcellulose prepared by melt extrusion—Part I. Int J Pharm 251:165–174.
17. Breitenbach J. 2002. Melt extrusion: From process to drug delivery technology. Eur JPharm Biopharm 54:107–117.
18. Patyi G, Bodis A, Antal I, Vajna B, Nagy ZK, Marosi G. 2010. Thermal and spectroscopic analysis of inclusion complex of spironolactone prepared by evaporation and hot melt methods. J Therm Anal Calorim 102:349–355.
19. Patyi G, Nagy Z, Vajna B, Anna P, Marosi G. 2012. Interfaces in multiphase polymers and nanomedicines. Materials Sci Forum 714:211–215.
20. Sauceau M, Fages J, Common A, Nikitine C, Rodier E. 2011. New challenges in polymer foaming: A review of extrusion processes assisted by supercritical carbon dioxide. Progr Polym Sci 36:749–766.
21. Verreck G, Decorte A, Heymans K, Adriaensen J, Cleeren D, Jacobs A, Liu D, Tomasko D, Arien A, Peeters J. 2005. The effect of pressurized carbon dioxide as a temporary plasticizer and foaming agent on the hot stage extrusion process and extrudate properties of solid dispersions of itraconazole with PVP-VA 64. Eur J Pharm Sci 26:349–358.
22. Nagy ZK, Sauceau M, Nyul K, Rodier E, Vajna B, Marosi G, Fages J. 2012. Use of supercritical CO_2-aided and conventional melt extrusion for enhancing the dissolution rate of an active pharmaceutical ingredient. Polym Adv Technol 23:909–918.
23. Vajna B, Pataki H, Nagy Z, Farkas I, Marosi G. 2011. Characterization of melt extruded and conventional Isoptin formulations using Raman chemical imaging and chemometrics. Int J Pharm 419:107–113.
24. Verreck G, Chun I, Peeters J, Rosenblatt J, Brewster ME. 2003. Preparation and characterization of nanofibers containing amorphous drug dispersions generated by electrostatic spinning. Pharm Res 20:810–817.
25. Yu DG, Zhang XF, Shen XX, Brandford-White C, Zhu LM. 2009. Ultrafine ibuprofen loaded polyvinylpyrrolidone fiber mats using electrospinning. Polym Int 58:1010–1013.
26. Yu DG, Shen XX, Branford-White C, White K, Zhu LM, Bligh S. 2009. Oral fast-dissolving drug delivery membranes prepared from electrospun polyvinylpyrrolidone ultrafine fibers. Nanotechnology 20:055104.
27. Yu DG, Yu JH, Chen L, Williams GR, Wang X. 2012. Modified coaxial electrospinning for the preparation of high-quality ketoprofen-loaded cellulose acetate nanofibers. Carbohydr Polym 90:1016–1023.
28. Nagy ZK, Nyul K, Wagner I, Molnar K, Marosi G. 2010. Electrospun water soluble polymer mat for ultrafast release of Donepezil HCl. Express Polym Lett 4:763–772.
29. Yu DG, Branford-White C, White K, Li XL, Zhu LM. 2010. Dissolution improvement of electrospun nanofiber-bsed solid dispersions for acetaminophen. AAPS PharmSciTech 11:809–817.
30. Nagy ZK, Balogh A, Vajna B, Farkas A, Patyi G, Kramarics Á, Marosi G. 2012. Comparison of electrospun and extruded soluplus-based solid dosage forms of improved dissolution. J Pharm Sci 101:322–332.
31. Nagy ZK, Patyi G, Bodzay B, Vajna B, Marosi G. 2011. Prüfungen und Herstellungsverfahren von Composites bis zu Nanomedikamenten. Gummi Fasern Kunststoffe 64:100–104.
32. Molnar K, Vas LM, Czigany T. 2012. Determination of tensile strength of electrospun single nanofibers through modeling tensile behavior of the nanofibrous mat. Composites B Eng 43:15–21.

33. Lukas D, Sarkar A, Martinova L, Vodsedalkova K, Lubasova D, Chaloupek J, Pokorny P, Mikes P, Chvojka J, Komarek M. 2009. Physical principles of electrospinning (electrospinning as a nano-scale technology of the twenty-first century). Textile Progr 41:59–140.
34. Yu D, Branford-White C, White K, Chatterton N, Zhu L, Huang L, Wang B. 2011. A modified coaxial electrospinning for preparing fibers from a high concentration polymer solution. Express Polym Lett 5:732–741.
35. Kostakova E, Meszaros L, Gregr J. 2009. Composite nanofibers produced by modified needleless electrospinning. Mater Lett 63:2419–2422.
36. Huang F, Wang Q, Wei Q, Gao W, Shou H, Jiang S. 2010. Dynamic wettability and contact angles of poly (vinylidene fluoride) nanofiber membranes grafted with acrylic acid. Express Polym Lett 4:551–558.
37. Rosic R, Kocbek P, Baumgartner S, Kristl J. 2011. Electrospun hydroxyethyl cellulose nanofibers: The relationship between structure and process. J Drug Deliv Sci Technol 21:229–236.
38. Sun K, Li Z. 2011. Preparations, properties and applications of chitosan based nanofibers fabricated by electrospinning. Express Polym Lett 5:342–361.
39. Rampichova M, Martinova L, Kostakova E, Filova E, Mickova A, Buzgo M, Michalek J, Pradny M, Necas A, Lukas D. 2012. A simple drug anchoring microfiber scaffold for chondrocyte seeding and proliferation. J Mater Sci 23:555–563.
40. Hutmacher DW, Dalton PD. 2011. Melt electrospinning. Chemistry 6:44–56.
41. Larrondo L, St John Manley R. 1981. Electrostatic fiber spinning from polymer melts. I. Experimental observations on fiber formation and properties. J Polym Sci Polym Phys Ed 19:909–920.
42. Zhou H, Green TB, Joo YL. 2006. The thermal effects on electrospinning of polylactic acid melts. Polymer 47:7497–7505.
43. Kim SJ, Jang DH, Park WH, Min BM. 2010. Fabrication and characterization of 3-dimensional PLGA nanofiber/microfiber composite scaffolds. Polymer 51:1320–1327.
44. Detta N, Brown TD, Edin FK, Albrecht K, Chiellini F, Chiellini E, Dalton PD, Hutmacher DW. 2010. Melt electrospinning of polycaprolactone and its blends with poly (ethylene glycol). Polym Int 59:1558–1562.
45. Ogata N, Shimada N, Yamaguchi S, Nakane K, Ogihara T. 2007. Melt-electrospinning of poly (ethylene terephthalate) and polyalirate. J Appl Polym Sci 105:1127–1132.
46. Wang X, Huang Z. 2010. Melt-electrospinning of PMMA. Chinese J Polym Sci 28:45–53.
47. Mitchell S, Sanders J. 2006. A unique device for controlled electrospinning. J Biomed Mater Res A 78:110–120.
48. Lyons J, Li C, Ko F. 2004. Melt-electrospinning part I: Processing parameters and geometric properties. Polym 45:7597–7603.
49. Malakhov S, Khomenko AY, Belousov S, Prazdnichnyi A, Chvalun S, Shepelev A, Budyka A. 2009. Method of manufacturing nonwovens by electrospinning from polymer melts. Fibre Chem 41:355–359.
50. Niu H, Lin T. 2012. Fiber generators in needleless electrospinning. J Nanomater 2012:13. doi:10.1155/2012/725950
51. Fang J, Zhang L, Sutton D, Wang X, Lin T. 2012. Needleless melt-electrospinning of polypropylene nanofibres. J Nanomater 2012:9. doi:10.1155/2012/382639
52. Wu JX, Yang M, Berg F, Pajander J, Rades T, Rantanen J. 2011. Influence of solvent evaporation rate and formulation factors on solid dispersion physical stability. Eur J Pharm Sci 44:610–620.
53. Rosic R, Pelipenko J, Kocbek P, Baumgartner S, Bester-Rogac M, Kristl J. 2012. The role of rheology of polymer solutions in predicting nanofiber formation by electrospinning. Eur Polym J 48:1374–1384.
54. Pataki H, Csontos I, Nagy ZK, Vajna B, Molnar M, Katona L, Marosi GJ. 2012. Implementation of Raman signal feedback to perform controlled crystallization of carvedilol. Org Process Res Dev [Epub ahead of print.] DOI: 10.1021/op300062t.
55. Pokharkar VB, Mandpe LP, Padamwar MN, Ambike AA, Mahadik KR, Paradkar A. 2006. Development, characterization and stabilization of amorphous form of a low Tg drug. Powder Technol 167:20–25.
56. Billes F, Pataki H, Unsalan O, Mikosch H, Vajna B, Marosi G. 2012. Solvent effect on the vibrational spectra of Carvedilol. Spectrochim Acta A Mol Biomol Spectrosc 95:148–164.
57. Patterson JE, James MB, Forster AH, Lancaster RW, Butler JM, Rades T. 2007. Preparation of glass solutions of three poorly water soluble drugs by spray drying, melt extrusion and ball milling. Int J Pharm 336:22–34.